# Advanced impedimetric biosensor configuration and assay protocol for glycoprofiling of a prostate oncomarker using Au nanoshells with a magnetic core

Tomas Bertok[a,b], Lenka Lorencova[a,b], Stefania Hroncekova[a], Veronika Gajdosova[a], Eduard Jane[a], Michal Hires[a], Peter Kasak[c], Ondrej Kaman[d], Roman Sokol[e], Vladimir Bella[f], Anita Andicsova Eckstein[g], Jaroslav Mosnacek[g], Alica Vikartovska[a], Jan Tkac[a,b,*]

[a] Institute of Chemistry, Slovak Academy of Sciences, Dubravska cesta 9, Bratislava 845 38, Slovak Republic
[b] Glycanostics Ltd., Dubravska cesta 9, Bratislava 845 38, Slovak Republic
[c] Center for Advanced Materials, Qatar University, P.O. Box 2713, Doha, Qatar
[d] Institute of Physics of the Czech Academy of Sciences, Cukrovarnicka 10/112, Prague 162 00, Czech Republic
[e] Private Urological Ambulance, Piaristicka 6, Trencin 911 01, Slovak Republic
[f] St. Elisabeth Cancer Institute, Heydukova 10, Bratislava 812 50, Slovak Republic
[g] Polymer Institute, Slovak Academy of Sciences, Dubravska cesta 9, Bratislava 845 41, Slovak Republic

## ARTICLE INFO

## ABSTRACT

In this paper several advances were implemented for glycoprofiling of prostate specific antigen (PSA), what can be applied for better prostate cancer (PCa) diagnostics in the future: 1) application of Au nanoshells with a magnetic core (MP@silica@Au); 2) use of surface plasmons of Au nanoshells with a magnetic core for spontaneous immobilization of zwitterionic molecules via diazonium salt grafting; 3) a double anti-fouling strategy with integration of zwitterionic molecules on Au surface and on MP@silica@Au particles was implemented to resist non-specific protein binding; 4) application of anti-PSA antibody modified Au nanoshells with a magnetic core for enrichment of PSA from a complex matrix of a human serum; 5) direct incubation of anti-PSA modified MP@silica@Au with affinity bound PSA to the lectin modified electrode surface. The electrochemical impedance spectroscopy (EIS) signal was enhanced 43 times integrating Au nanoshells with a magnetic core compared to the biosensor without them. This proof-of-concept study shows that the biosensor could detect PSA down to 1.2 fM and at the same time to glycoprofile such low PSA concentration using a lectin patterned biosensor device. The biosensor offers a recovery index of 108%, when serum sample was spiked with a physiological concentration of PSA (3.5 ng mL$^{-1}$).

## 1. Introduction

Prostate cancer (PCa) is the most commonly diagnosed cancer type among men in 92 countries (1 in 7 men will be diagnosed with PCa in their lifetime) (Saman et al., 2014) and one of the most prevalent cancer types in general (Torre et al., 2015). PCa is diagnosed to 1.1 million men with estimated number of deaths of 307,500 each year (Torre et al., 2015) with a projected increase of incidence to 2.1 million by 2035 with up to 633,328 associated deaths (O'Reilly and O'Kennedy, 2017). One study even suggests that in 100 years, 50% of all men will be diagnosed with PCa in their lifetime (Pollock et al., 2015) due to significant aging of population (Moraga-Serrano, 2018).

The most commonly utilized PCa oncomarker – prostate specific antigen (PSA) is not a tumor specific, but rather a prostate specific (Ablin, 2014; Ablin and Piana, 2014). This means that elevated PSA level in the blood is observed after disruption of the basement membrane of the prostate gland as result of prostate inflammation and other conditions besides PCa. The discoverer of PSA, a pathologist Richard Ablin is against the use of PSA as a diagnostic PCa biomarker nor as a PCa prognostic biomarker (i.e. to distinguish indolent from aggressive PCa), but rather suggests to use PSA as an indicator of disease recurrence (Ablin, 2014; Ablin and Piana, 2014).

PSA test provides quite high false-positive rate (up to ∼75%) (Garnick et al., 2018) meaning that 75% of subsequently performed biopsies are avoidable with a significant burden on men, society and healthcare system. In addition, 15–17% of men with normal PSA level

(*i.e.* up to 4 ng mL$^{-1}$) already have PCa (Garnick et al., 2018) and the disease can develop into an advanced and life-threating stage. The controversy behind using PSA for PCa diagnostics could be documented by the following facts: 1. US Food and Drug Administration (FDA) agency approved PSA tests together with digital rectal examination (DRE) for PCa diagnostics in 1994 (O'Reilly and O'Kennedy, 2017); 2. due to PCa overdiagnosis, the US Preventative Services Task Force (USPSTF) published a recommendation against the use of PSA for PCa diagnosis in 2012 (Moyer, 2012); 3. since publication of this recommendation a more advanced PCa with a higher proportion of tumors of higher grade and stage was detected (Fleshner et al., 2017) and this is why in 2017, the USPSTF recommended selective use of PSA tests for men aged from 55 to 70 (Grossman et al., 2018; Van Der Kwast and Roobol, 2017).

A robust and accurate early stage PCa diagnostics with low false negative rate and false positive rate is required. Survival is proportional to stage at diagnosis and thus early stage diagnostics using disruptive and effective diagnostic tools is a key to reduce mortality. At the same time low false positive rate will decrease number of avoidable biopsies to minimum. Thus, we really need novel types of PCa biomarkers for PCa diagnostics. There are several PCa biomarkers currently under development and clinical validation (Bravaccini et al., 2018; Yao et al., 2018; Zhang et al., 2017) with few of them such as PHI and 4 K score tests already approved by regulatory agencies (O'Reilly and O'Kennedy, 2017; Rodríguez and O'Kennedy, 2017; Sharma et al., 2017). A pioneering study suggests that besides traditional biomarkers (Cohen et al., 2018), glycans (complex carbohydrates) can have significant clinical performance as novel PCa biomarkers (Murphy et al., 2018).

Traditional glycan analysis performed by instrumental methods has some drawbacks and a limited utility in a clinical practice (Dosekova et al., 2017; Tkac et al., 2019a). This is why we have used lectins (proteins specifically recognizing glycans) for development of electrochemical biosensors for detection of glycan changes directly on the PSA protein (Belicky et al., 2017; Pihikova et al., 2016a, 2016b, 2016c). Detection of changes in the glycosylation pattern of PSA protein using lectins is a powerfull strategy applicable for diagnostics and prognostics of PCa (Fukushima et al., 2010; Tkac et al., 2019a, 2019b). Since interaction between glycans and lectins is much weaker compared to antigen-antibody affinity pair, it is of high importance to ensure multiple binding points between lectins and glycans. In this study we applied Au nanoshells with a magnetic core (Kaman et al., 2017a, 2017b) covered by antibodies for selective PSA enrichment from serum with subsequent presentation of such particles to an electrode modified by a lectin for high performance glycoprofiling of PSA (Scheme 1).

## 2. Experimental section

Reagents and apparatus used are described in the Supp. info file.

### 2.1. Real human samples

Single serum sample from a healthy woman individual (essentially free of any PSA) was used in the study. The subject gave an informed written consent, and the study was approved by the Ethical Committee of the St. Elisabeth Cancer Institute in Bratislava, Slovakia in an agreement with the ethical guidelines of the Declaration of Helsinki as revised in 2013. Blood sample was collected into a standard serum tube with a silicone-coated interior (BD Vacutainer, Franklin Lakes, NJ USA), clotted at a room temperature (RT) for approximately 1 h, and subsequently the serum was transferred into separate sterile tubes and stored at −80 °C until use.

### 2.2. Synthesis of MP@silica@Au particles and TEM/DLS characterization

The particles composed of Mn-Zn ferrite cores, primary silica coating and secondary gold nanoshell were prepared by a multistep procedure that involved hydrothermal synthesis of $Mn_{0.61}Zn_{0.42}Fe_{1.97}O_4$ nanocrystalites (Kaman et al., 2017b), their encapsulation into silica by the poly(vinylpyrrolidone) (PVP) method (Graf et al., 2003), and deposition of gold nanoshell by a seed-and-growth method (Koktan et al., 2017). The whole procedure was described in the previous report, and the full details can be found in the accompanying paper (Bertok et al., 2019b). DLS experiment of bare MP@silica@Au particles revealed a hydrodynamic radius of 271 ± 19 nm. This suggests a slight aggregation, thus a mild sonication step (6 × 10 s) was applied *prior* to modification of the surface. TEM images of the prepared MP@silica@Au particles are shown in Fig. 1. XRD pattern of $Mn_{0.61}Zn_{0.42}Fe_{1.97}O_4$ particles and TEM images of MP@silica particles are provided elsewhere (Bertok et al., 2019b).

### 2.3. Synthesis of zwitterionic diazonium compounds and characterization

Synthesis of *tert*-butyl 4-((dimethylamino)methyl)phenylcarbamate and subsequent syntheses of carboxybetaine (CB) and sulfobetaine (SB) derivatives together with relevant schemes and $^1$H NMR and $^{13}$C NMR spectra can be found in Bertok et al. (2019b). Shortly, the CB and SB aryldiazonium derivatives were synthesized according to the Scheme 2.

### 2.4. Surface modifications using zwitterionic derivatives

Gold electrodes surface modification was performed according to a slightly modified, previously published protocol (Li et al., 2014). Shortly, 59 mM protected diazonium salt solution in deionized water (DW) (1 equivalent) was mixed with 4 equivalents of HBF$_4$ in acetonitrile at RT for 45 min in dark. Subsequently, 1.1 equivalent of *tert*-butyl nitrite was added dropwise to the mixture on ice and the solution was mixed for 2 h at RT. The final solution was subsequently diluted to obtain 2 mM solution of zwitterionic aryldiazonium salt derivative and cyclic voltammetry (from 0.0 V to −1.0 V at a scan rate of 0.25 V s$^{-1}$ for 24 cycles) was applied to obtain SAM layer on an Au electrode surface. The reason for activating diazonium salt just *prior* to its immobilization is the fact that the molecule is not stable for a longer period of time. Since MP@silica@Au particles having outer golden shell have free surface plasmons, the particle modification do not need to involve
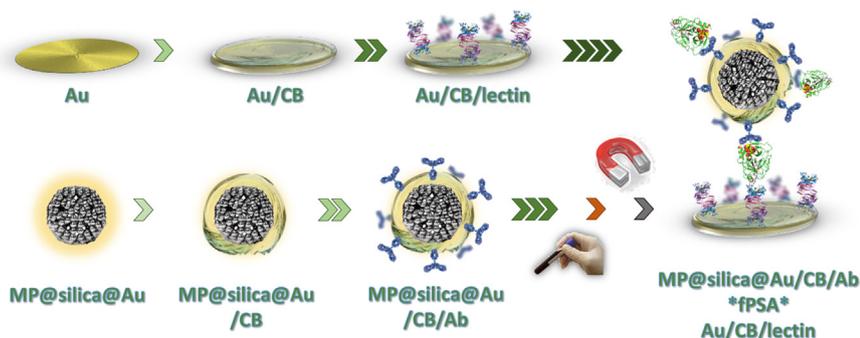


**Scheme 1.** Modification of Au electrode (upper row) using carboxybetaine aryldiazonium derivative (CB) and lectin (SNA-I). In the first step, carboxybetaine-bearing SAM layer was formed using cyclic voltammetry, and subsequently served for the covalent immobilization of a lectin. Lower row shows MP@silica@Au composite spontaneously modified with CB-derivative and subsequently with an antibody (Ab, anti-fPSA, chemically treated). After enrichment of fPSA from human sample using MP@silica@Au/CB/Ab by a permanent magnet, a sandwich was prepared and the signal was evaluated electrochemically.
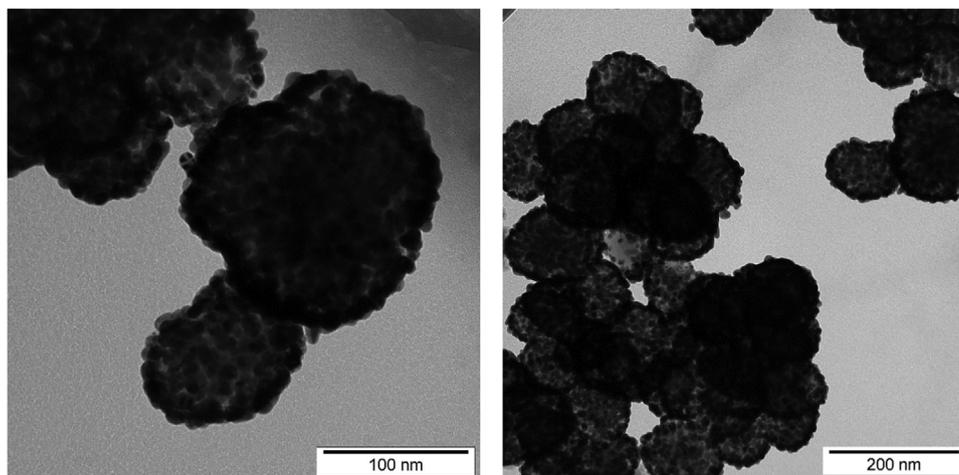
**Fig. 1.** TEM images of the MP@silica@Au clusters synthesized and subsequently used for diazonium-derived zwitterionic SAM layer modification and anti-fPSA immobilization for selective PSA enrichment at different zoom.

electrochemical grafting and proceed spontaneously. Subsequently, SAM layers prepared this way were further modified using amine coupling chemistry (0.2 M EDC and 0.05 M NHS in 1 + 1 ratio for 15 min) by anti-fPSA (Au nanoshells with a magnetic core) and SNA-I lectin (Au electrode) for enrichment and biorecognition, respectively.

### 2.5. Chemical oxidation of antibody´s glycan

Glycan present on anti-PSA antibody was oxidized by using a slightly modified mild chemical oxidation procedure as described previously (Chen et al., 2007). Shortly, monoclonal anti-fPSA (c = 2 mg mL$^{-1}$) was diluted by 150 mM NaIO$_4$ in 150 mM sodium acetate pH 5.5 solution down to 0.1 mg mL$^{-1}$ and incubated in the dark for 30 min at 4 °C. After a desalting procedure with previously equilibrated desalting columns (Zeba spin 7 K MWCO, Thermo Scientific), 2 mM solution of propionic acid hydrazide in 150 mM sodium acetate pH 5.5 was added to the oxidized anti-fPSA in 1 + 1 ratio. The mixture was incubated in the dark for 2 h at RT. After the desalting procedure, the oxidized anti-fPSA (with concentration of 0.05 mg mL$^{-1}$) was stored in the form of aliquots at −80 °C. Standard enzyme-linked lectin binding assay (ELLBA, according to protocols published in our previous work (Chocholova et al., 2018a; Chocholova et al., 2018b) revealed successful glycan oxidation and its modification by propionic acid

hydrazide suppressing lectin binding.

### 2.6. Electrochemical characterization and measurements

Gold electrodes (d = 1.6 mm, BASi, Bioanalytical Systems, USA) were pretreated and regenerated as described previously (Bertok et al., 2015). Various types of electrochemical techniques were applied for calculation of real electrode surface (effective surface area), interfacial surface coverage of zwitterionic derivatives on Au electrodes and for fPSA detection. Density of zwitterionic aryldiazonium derivatives on gold electrodes was calculated using a reductive desorption (CV from −0.5 V to −1.5 V at a scan rate of 0.1 V s$^{-1}$ for 75 scans) in 0.1 M NaOH, under N$_2$ atmosphere. The effective electrode surface area was calculated from CV run from -0.1 V to 0.6 V in 5 mM solution of ferri/ferrocyanide in 0.1 M PB (pH 7.0), scan rate ranging from 0.1 to 0.5 V s$^{-1}$ for five consecutive scans (with each new scan, the step in scan rate increased by 0.1 V s$^{-1}$) and Randles-Sevcik equation (Eq. 1, where *n* is the number of electrons transferred, $A_{EFF}$ is the electrode area or effective area, *D* is diffusion coefficient, *C* is the bulk concentration and *v* is the scan rate). Electrochemical impedance spectroscopy (EIS) measurements were run in ferri/ferrocyanide solution in 0.1 M PB (pH 7.0) *vs.* OCP at 50 different frequencies ranging from 0.1 Hz to 100 kHz, with charge transfer resistance (R$_{CT}$, semicircle diameter in Nyquist
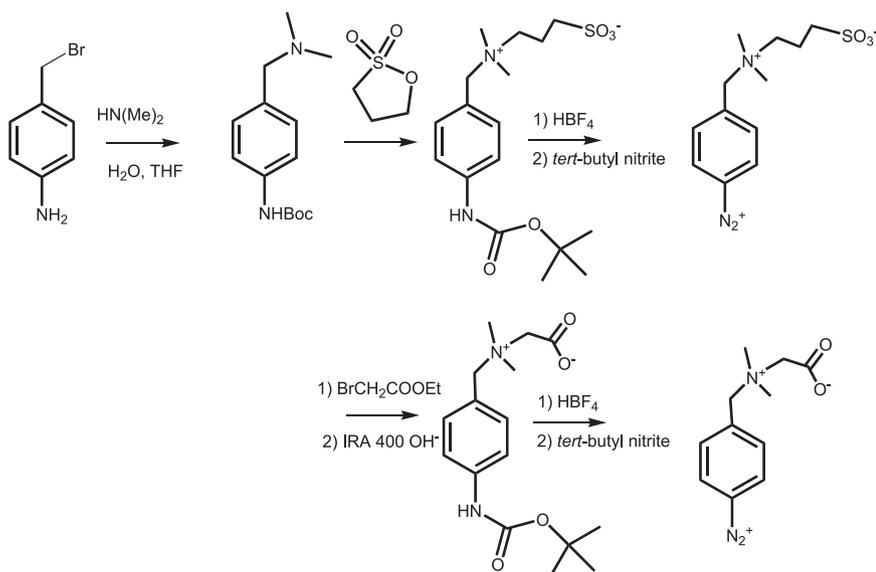


**Scheme 2.** Synthesis of zwitterionic SB and CB derivatives; *tert*-butyl 4-(bromomethyl)phenylcarbamate was used for alkylation of dimethylamine to form dimethylamino derivative. For the synthesis of sulfobetaine the resulting tertiary amine was let to react with 1,3-propane sultone and to form a zwitterion, that was (the same way as carboxybetaine) *in situ* deprotected under acidic conditions and formed diazonium salt for the reaction with an electrode surface using a negative potential window scanning. The analogous synthesis of the carboxybetaine derivative is shown in the lower part of this Scheme.

plot) being the signal obtained and R(Q[RW]) being the circuit used for fitting the raw data. All incubation steps of particles with a sample (*i.e.* PSA spiked in a serum sample during the enrichment step) or particles with immobilized PSA with electrode interface took 15 min. After the PSA enrichment, MP@silica@Au particles were subsequently isolated using a permanent neodymium magnet and gently washed twice using phosphate buffer.

$$i_p = 268,600 \quad n^{\frac{3}{2}} A_{EFF} D^{\frac{1}{2}} C v^{\frac{1}{2}} \tag{1}$$

## 3. Results and discussion

### 3.1. Formation of zwitterionic SAM on gold and its characterization

Planar gold electrodes exhibit effective surface area of 3.7 mm² (*i.e.* ~46% higher compared to a geometrical electrode surface area) and the surface coverage of carboxybetaine derivative was 2.1 molecules nm⁻². The latter value is in an excellent agreement with the previously published value for sulfobetaine derivative of thiooctic acid on gold (1.97 molecules nm⁻²) (Bertok et al., 2013), or for thiooctic acid on gold surface (1.8–2.1 molecules nm⁻²) (Volkert et al., 2011).

For the aryldiazonium salt-based SAM layer preparation, it is crucial to use freshly prepared diazonium derivative solution, as well as freshly regenerated gold electrodes. FT-IR spectra revealed, that in water phase and at RT, the diazonium $-N^+ \equiv N$ group is completely changed to hydroxylic −OH group within 1 h (Bertok et al., 2019b). This is the reason why yields of diazonium salts preparation reactions published are usually 65–67% (Derible et al., 2014). According to what is commonly found in the literature, peak representing the $-N^+ \equiv N$ group is found between 2200 and 2300 cm⁻¹ (Yang et al., 2012), while we observed a new peak at 2620 cm⁻¹, which is in the −O-H stretch region (SB precursor molecule did not contain any hydroxylic groups). Moreover, we indirectly confirmed the formation of diazonium derivative from the precursor by observing the SAM layer formation on gold, as in the case of QCM crystal modified using sulfobetaine aryldiazonium derivative (Li et al., 2014).

NMR spectra of the synthesized precursors for carboxy- and sulfo-betaine aryldiazonium derivatives can be found in (Bertok et al., 2019b). Besides having a peak at ~-0.9 V *vs.* Ag/AgCl (Fig. 2 left) in CV during formation of SAM (Li et al., 2014), another proof for a newly formed layer is change of the interfacial wetting (contact) angle, *i.e.* change in the wettability of the surface (Fig. 2 right). In case of both CB or SB aryldiazonium derivatives, the surface became much more

hydrophilic (61° for CB and 43° for SB) due to the presence of both positive and negative charges on the interface, when compared to bare Au electrode (88°). Additional XPS measurements of modified Au surfaces are in (Bertok et al., 2019b).

Moreover, we did also a combined electrochemical QCM experiment with CV run during such an experiment. The results indicated change in the frequency during SAM layer formation of 12.2 Hz, when a stable CV was reached (Fig. 2 left). According to the Sauerbrey´s equation (Eq. 2, where $\Delta f$ is the frequency change [Hz], $f_0$ is the nominal resonant frequency of the crystal [6 MHz], $\Delta m$ is the change in mass [g cm⁻²] and $\mu_q$ is the shear modulus of a quartz [g cm⁻¹ s⁻²], $A$ is the surface area and $q$ is density of quartz in g mL⁻¹), a value of 149 ng cm⁻² was obtained, what for a CB derivative (with Mw = 372.17 g mol⁻¹) leads to a surface coverage of 2.4 molecules nm⁻², a value in a good agreement with the result obtained by a reductive desorption experiment (2.1 molecules nm⁻², see above). The result is in a good agreement with density of thiolated ferrocene chemisorbed on gold at density of 2.4–2.6 molecules nm⁻² (Shimazu et al., 1992).

$$\Delta f = -\frac{2f_0^2}{A\sqrt{\rho_q \mu_q}} \Delta m = -C_f \Delta m \, (C_f = 0.0815 Hz \, ng^{-1} cm^2) \tag{2}$$

### 3.2. Biosensor construction and characterization

The results indicate that CB has beneficial properties over SB since CB is able to more significantly resist non-specific interactions over CB (Fig. S1 in Supporting information file) and at the same time CB contains −COOH functional groups applicable for covalent immobilization of antibodies and lectins. In our recent review paper (Bertok et al., 2019a), we stated that the dominant challenge of EIS-based biosensors is to address non-specific binding of proteins since the level of highly abundant proteins such as albumin is present in 10⁷-fold higher concentrations compared to PSA in human sera) may interfere dramatically with the assay (Bertok et al., 2019a). In this study, this problem was addressed by a double anti-fouling strategy based on a sandwich formed between lectin immobilized on a CB-modified Au surface and anti-PSA covalently linked on CB-modified MP@silica@Au particles. This design allows us to specifically bind PSA from diluted sera (with minimal non-specific adsorption), separate and wash the particles and use them for the interaction with the biosensor´s surface. Moreover, CB with diazonium functionality can be effectively applied not only to pattern gold electrodes, but any conductive surface including disposable and low-cost electrodes such as screen-printed electrodes. Thus, in the future it
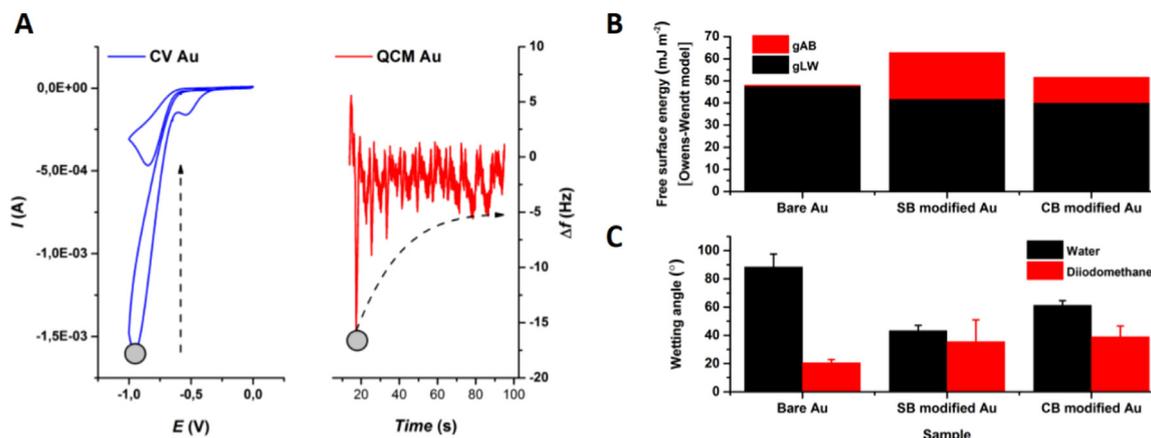


**Fig. 2.** EQCM of the preparation of zwitterionic SAM layer (A). A reduction peak occurs and decreases with each cycle at ~-0.9 V *vs.* Ag/AgCl (1st and 24th scan, grey circle shows the 1st scan reduction moment). Wetting angle (WA) measurement (B,C) using a two-liquid system with DW and diiodomethane. Free surface energy (B) was calculated using Owens-Wendt model. Bare Au electrode after polishing and gold oxide stripping procedure was strongly hydrophobic (WA ~88° in DW). After the formation of CB/SB SAM layer, the interface becomes more hydrophilic with an increase in the polar component of the free surface energy due to the presence of zwitterions (C).
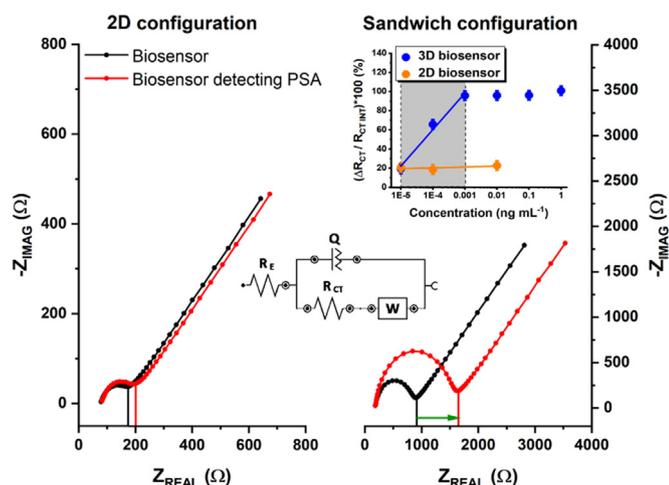
**Fig. 3.** The representative Nyquist plots for common 2D configuration (planar electrode interface modified using SAM layer and anti-fPSA antibody (left) and a sandwich-based configuration using MP@silica@Au clusters modified with anti-fPSA with an electrode modified using SNA-I lectin (right). EIS data were fitted using [R(Q[RW])] equivalent circuit (as showed in the inset). A response towards $0.1\,\text{ng}\,\text{mL}^{-1}$ PSA in $10\times$ diluted real human serum is shown (red curves). A calibration curve for fPSA (blue) for a sandwich configuration is shown in the inset (error bars are too small to be visible). According to the slopes of calibration curves in the linear response range for both configurations, an amplification factor of 43 was calculated. (For interpretation of the references to color in this figure legend, the reader is referred to the web version of this article.)

is possible to prepare electrochemical array biosensor set-up for detection of multiple oncomarkers in a single sample.

The other beneficial role of using MP@silica@Au is a significantly amplified EIS response. The biosensor integrating MP@silica@Au offers dramatically larger shift of $R_{CT}$ (sandwich configuration, 3D biosensor), when compared to the biosensor device without using such particles (2D biosensor) (Fig. 3) for detection of $0.1\,\text{ng}\,\text{mL}^{-1}$ PSA. Moreover, the slope of the calibration curve for PSA detection within linear range ($0.01–1\,\text{pg}\,\text{mL}^{-1}$) using MP@silica@Au particles was $43\times$ larger, when compared to the device without using such particles (Fig. 3 inset). The curve reached the saturation already at the concentration of $0.001\,\text{ng}\,\text{mL}^{-1}$ and from the calibration curve we calculated LOD as $34\,\text{fg}\,\text{mL}^{-1}$ (*i.e.* $= 1.2\,\text{fM}$) (S/N = 3). The biosensor presented in this study belongs to the one of the most sensitive devices for detection of PSA published so far (Damborska et al., 2017; Shi et al., 2018). The most recent studies described electrochemical devices with LOD down to $1\,\text{fg}\,\text{mL}^{-1}$ (Tang et al., 2017); $10\,\text{fg}\,\text{mL}^{-1}$ (Kukkar et al., 2017), $120\,\text{fg}\,\text{mL}^{-1}$ (Zhou et al., 2018), $3\,\text{pg}\,\text{mL}^{-1}$ (Chen et al., 2019; Han et al., 2018), $10\,\text{pg}\,\text{mL}^{-1}$ (Wei et al., 2018), $17\,\text{pg}\,\text{mL}^{-1}$ (Shi et al., 2018) and devices based on other detection schemes with LOD down to $1\,\text{pg}\,\text{mL}^{-1}$ (Chinnadayyala et al., 2019) or $20\,\text{pg}\,\text{mL}^{-1}$ (Gao et al., 2019). The biosensor device presented here does not only belong to one of the most sensitive biosensor devices described so far, but the presented assay concept is advantageous since it allows to glycoprofile PSA from a complex samples and the assay concept can be easily integrated into an array format. Finally, the biosensor was applied in analysis of PSA spiked into $10\times$ diluted female serum sample. When the physiological concentration of PSA ($3.5\,\text{ng}\,\text{mL}^{-1}$) was spiked into the serum sample, the recovery index of 108% was obtained underlining robust biosensor performance in such complex sample.

## 4. Conclusions

In this study, we focused our effort to develop a sensitive, reliable and label-free detection of fPSA in human sera. The Au nanoshells with a magnetic core MP@silica@Au applied in the study have triple role - 1.

enrichment of PSA from a complex serum sample, 2. amplification of the EIS response by a factor of 43 and 3. presentation of multiple PSA´s glycans to the immobilized lectin making such interaction stronger. In order to resist non-specific protein binding, a double anti-fouling strategy based on a sandwich formed between lectin immobilized on a CB-modified Au surface and anti-PSA covalently linked on CB-modified MP@silica@Au particles was implemented. We believe that our proof of concept PSA glycoprofiling assay format is scalable for analysis of other glycans present on PSA of for glycoprofiling of other cancer biomarkers and that the assay protocol can be easily integrated into a multiplexed format of analysis of oncomarkers.

editing

Ondrej Kaman: conceptualization, data curation, investigation, visualization, methodology, writing - original draft, writing - review and editing

Roman Sokol: conceptualization, resources, supervision

Vladimir Bella: conceptualization, resources, supervision, validation, writing - original draft

Anita Andicsova Eckstein: data curation, investigation, methodology,

Jaroslav. Mosnacek: data curation, investigation, methodology, funding acquisition, supervision, writing - original draft

Alica Vikartovska: data curation, fomal analysis, investigation, visualization, project administration

Jan Tkac: conceptualization, formal analysis, funding acquisition, project administration, validation, supervison, visualization, writing - original draft, writing - review and editing

## Declaration of interests

The authors declare that they have no known competing financial interests or personal relationships that could have appeared to influence the work reported in this paper.

## Appendix A. Supporting information

Supplementary data associated with this article can be found in the online version at https://doi.org/10.1016/j.bios.2019.01.052.

## References

Ablin, R.J., 2014. Prostate cancer test has been misused for money. The Scientist (internet version):, ⟨https://www.newscientist.com/article/mg22129564-400-prostate-cancer-test-has-been-misused-for-money/⟩.

Ablin, R.J., Piana, R., 2014. The Great Prostate Hoax: How Big Medicine Hijacked the PSA Test and Caused A Public Health Disaster. Palgrave McMillian, United States.

Belicky, S., Damborsky, P., Zapatero-Rodriguez, J., O'Kennedy, R., Tkac, J., 2017. Electrochim. Acta 246, 399–405.

Bertok, T., Klukova, L., Sediva, A., Kasák, P., Semak, V., Micusik, M., Omastova, M., Chovanová, L., Vlček, M., Imrich, R., 2013. Anal. Chem. 85, 7324--77332.

Bertok, T., Lorencova, L., Chocholova, E., Jane, E., Vikartovska, A., Kasak, P., Tkac, J., 2019a. ChemElectroChem. https://doi.org/10.1002/celc.201800848.

Bertok, T., Lorencova, L., Hroncekova, S., Gajdosova, V., Jane, E., Hires, M., Kasak, P., Kaman, O., Sokol, R., Bella, V., Andicsova Eckstein, A., Mosnacek, J., Vikartovska, A., Tkac, J., 2019b. MethodsX.

Bertok, T., Šedivá, A., Filip, J., Ilcikova, M., Kasak, P., Velic, D., Jane, E., Mravcová, M., Rovenský, J., Kunzo, P., 2015. Langmuir 31, 7148--77157.

Bravaccini, S., Puccetti, M., Bocchini, M., Ravaioli, S., Celli, M., Scarpi, E., De Giorgi, U., Tumedei, M.M., Raulli, G., Cardinale, L., 2018. Sci. Rep. 8, 4254.

Chen, S., LaRoche, T., Hamelinck, D., Bergsma, D., Brenner, D., Simeone, D., Brand, R.E., Haab, B.B., 2007. Nat. Methods 4, 437–444.

Chen, Y., Yuan, P.-X., Wang, A.-J., Luo, X., Xue, Y., Zhang, L., Feng, J.-J., 2019. Biosens. Bioelectron. 126, 187–192.

Chinnadayyala, S.R., Park, J., Le, H.T.N., Santhosh, M., Kadam, A.N., Cho, S., 2019. Biosens. Bioelectron. 126, 68–81.

Chocholova, E., Bertok, T., Jane, E., Lorencova, L., Holazova, A., Belicka, L., Belicky, S., Mislovicova, D., Vikartovska, A., Imrich, R., Kasak, P., Tkac, J., 2018a. Clin. Chim. Acta 481, 49–55.

Chocholova, E., Bertok, T., Lorencova, L., Holazova, A., Farkas, P., Vikartovska, A., Bella, V., Velicova, D., Kasak, P., Eckstein, A.A., Mosnacek, J., Hasko, D., Tkac, J., 2018b. Sens. Actuators B: Chem. 272, 626–633.

Cohen, J.D., Li, L., Wang, Y., Thoburn, C., Afsari, B., Danilova, L., Douville, C., Javed,

A.A., Wong, F., Mattox, A., 2018. Science eaar3247.

Damborska, D., Bertok, T., Dosekova, E., Holazova, A., Lorencova, L., Kasak, P., Tkac, J., 2017. Microchim. Acta 184, 3049–3067.

Derible, A., Diebold, C., Dentzer, J., Gadiou, R., Becht, J.M., Le Drian, C., 2014. Eur. J. Org. Chem. 2014, 7699–7706.

Dosekova, E., Filip, J., Bertok, T., Both, P., Kasak, P., Tkac, J., 2017. Med. Res. Rev. 37, 514–626.

Fleshner, K., Carlsson, S.V., Roobol, M.J., 2017. Nat. Rev. Urol. 14, 26–37.

Fukushima, K., Satoh, T., Baba, S., Yamashita, K., 2010. Glycobiology 20, 452–460.

Gao, Y., Huo, W., Zhang, L., Lian, J., Tao, W., Song, C., Tang, J., Shi, S., Gao, Y., 2019. Biosens. Bioelectron. 123, 204–210.

Garnick, M.B., Abrahamsson, P.-A., Dewolf, W.C., Kacker, R., Kaplan, I., Louglin, K.R., Srougi, M., Sternberg, C.N., Zietman, A.L., 2018. Harvard Medical School 2018 Annual Report on Prostate Diseases. Harvard Health Publishing, Boston.

Graf, C., Vossen, D.L., Imhof, A., van Blaaderen, A., 2003. Langmuir 19, 6693–6700.

Grossman, D.C., Curry, S.J., Owens, D.K., Bibbins-Domingo, K., Caughey, A.B., Davidson, K.W., Doubeni, C.A., Ebell, M., Epling Jr, J.W., Kemper, A.R., Krist, A.H., Kubik, M., Landefeld, C.S., Mangione, C.M., Silverstein, M., Simon, M.A., Siu, A.L., Tseng, C.-W., 2018. JAMA 319, 1901–1913.

Han, L., Xia, H., Yin, L., Petrenko, V.A., Liu, A., 2018. Biosens. Bioelectron. 106, 1–6.

Kaman, O., Kuličková, J., Herynek, V., Koktan, J., Maryško, M., Dědourková, T., Knížek, K., Jirák, Z., 2017a. J. Magn. Magn. Mater. 427, 251–257.

Kaman, O., Kuličková, J., Maryško, M., Veverka, P., Herynek, V., Havelek, R., Královec, K., Kubániová, D., Kohout, J., Dvořák, P., 2017b. IEEE Trans. Magn. 53. https://doi.org/10.1109/TMAG.2017.2721365.

Koktan, J., Královec, K., Havelek, R., Kuličková, J., Řezanka, P., Kaman, O., 2017. Colloids Surf. A 520, 922–932.

Kukkar, M., Singh, S., Kumar, N., Tuteja, S.K., Kim, K.-H., Deep, A., 2017. Microchim. Acta 184, 4647–4654.

Li, B.-R., Shen, M.-Y., Yu, H.-H., Li, Y.-K., 2014. Chem. Commun. 50, 6793–6796.

Moraga-Serrano, P.E., 2018. JAMA Oncol. ⟨http://eprints.lancs.ac.uk/id/eprint/126049⟩.

Moyer, V.A., 2012. Ann. Intern. Med. 157, 120–134.

Murphy, K., Murphy, B.T., Boyce, S., Flynn, L., Gilgunn, S., O'Rourke, C.J., Rooney, C., Stöckmann, H., Walsh, A.L., Finn, S., O'Kennedy, R.J., O'Leary, J., Pennington, S.R., Perry, A.S., Rudd, P.M., Saldova, R., Sheils, O., Shields, D.C., Watson, R.W., 2018. Mol. Oncol. 12, 1513–1525.

O'Reilly, J.-A., O'Kennedy, R.J., 2017. J. Cancer Treat. Diagn. 2, 18–25.

Pihikova, D., Belicky, S., Kasak, P., Bertok, T., Tkac, J., 2016a. Analyst 141, 1044–1051.

Pihikova, D., Kasak, P., Kubanikova, P., Sokol, R., Tkac, J., 2016b. Anal. Chim. Acta 934, 72–79.

Pihikova, D., Pakanova, Z., Nemcovic, M., Barath, P., Belicky, S., Bertok, T., Kasak, P., Mucha, J., Tkac, J., 2016c. Proteomics 16, 3085–3095.

Pollock, P., Ludgate, A., Wassersug, R., 2015. Curr. Oncol. 22, 10.

Rodríguez, J.Z., O'Kennedy, R., 2017. Asian Hosp. Healthc. Manag 18–23.

Saman, D.M., Lemieux, A.M., Lutfiyya, M.N., Lipsky, M.S., 2014. Dis. Mon. 60, 150–154.

Sharma, S., Zapatero-Rodríguez, J., O'Kennedy, R., 2017. Biotechnol. Adv. 35, 135–149.

Shi, Y.-C., Wang, A.-J., Yuan, P.-X., Zhang, L., Luo, X., Feng, J.-J., 2018. Biosens. Bioelectron. 111, 47–51.

Shimazu, K., Yagi, I., Sato, Y., Uosaki, K., 1992. Langmuir 8, 1385–1387.

Tang, Z., Fu, Y., Ma, Z., 2017. Biosens. Bioelectron. 94, 394–399.

Tkac, J., Bertok, T., Hires, M., Jane, E., Lorencova, L., Kasak, P., 2019a. Exp. Rev. Proteom. 16, 65–76.

Tkac, J., Gajdosova, V., Hroncekova, S., Bertok, T., Hires, M., Jane, E., Lorencova, L., Kasak, P., 2019b. Interface Focus. https://doi.org/10.1098/rsfs.2018.0077.

Torre, L.A., Bray, F., Siegel, R.L., Ferlay, J., Lortet-Tieulent, J., Jemal, A., 2015. CA: Cancer J. Clin. 65, 87–108.

Van Der Kwast, T.H., Roobol, M.J., 2017. Nat. Rev. Urol. 14, 457–458.

Volkert, A.A., Subramaniam, V., Ivanov, M.R., Goodman, A.M., Haes, A.J., 2011. ACS Nano 5, 4570–4580.

Wei, B., Mao, K., Liu, N., Zhang, M., Yang, Z., 2018. Biosens. Bioelectron. 121, 41–46.

Yang, Y., Song, X., Yuan, L., Li, M., Liu, J., Ji, R., Zhao, H., 2012. J. Polym. Sci. Part A: Polym. Chem. 50, 329–337.

Yao, J., Wang, Y., Dai, Y., Liu, C.C., 2018. ACS Omega 3, 6411–6418.

Zhang, A.Y., Grogan, J.S., Mahon, K.L., Rasiah, K., Sved, P., Eisinger, D.R., Boulas, J., Vasilaris, A., Henshall, S.M., Stricker, P.D., Kench, J.G., Horvath, L.G., 2017. Ann. Oncol. 28, 1903–1909.

Zhou, X., Yang, L., Tan, X., Zhao, G., Xie, X., Du, G., 2018. Biosens. Bioelectron. 112, 31–39.